

## REVEALING A COOL ACCRETION DISK IN THE ULTRALUMINOUS X-RAY SOURCE M81 X-9 (HOLMBERG IX X-1): EVIDENCE FOR AN INTERMEDIATE-MASS BLACK HOLE

J. M. MILLER,<sup>1,2</sup> A. C. FABIAN,<sup>3</sup> AND M. C. MILLER<sup>4</sup>

Received 2003 October 21; accepted 2004 February 12

### ABSTRACT

We report the results of an analysis of two *XMM-Newton* EPIC-pn spectra of the bright ultraluminous X-ray source M81 X-9 (Holmberg IX X-1) obtained in snapshot observations. Soft thermal emission is clearly revealed in spectra dominated by hard power-law components. Depending on the model used, M81 X-9 was observed at a luminosity of  $L_X = (1.0\text{--}1.6) \times 10^{40}$  ergs  $s^{-1}$  (0.3–10.0 keV). The variability previously observed in this source signals that it is an accreting source that likely harbors a black hole. Remarkably, accretion disk models for the soft thermal emission yield very low inner disk temperatures ( $kT = 0.17\text{--}0.29$  keV, including 90% confidence errors and variations between observations and disk models) and improve the fit statistic over any single-component continuum model at the  $6\sigma$  level of confidence. This represents much stronger evidence for a cool disk than prior evidence that combined spectra from different observatories, and the strongest evidence of a cool disk in an ultraluminous X-ray source apart from that for NGC 1313 X-1. In common with NGC 1313 X-1, scaling the temperatures measured in M81 X-9 to those commonly seen in stellar-mass Galactic black holes at their highest observed fluxes ( $kT \simeq 1$  keV) may imply that M81 X-9 harbors a black hole with a mass on the order of  $10^3 M_\odot$ ; the measured disk component normalization and broadband luminosity imply black hole masses on the order of  $10^2 M_\odot$ . It is therefore possible that these sources harbor  $10^3 M_\odot$  black holes accreting at  $L_X \simeq 0.1 \times L_{\text{Edd}}$ . While these results do not represent proof that M81 X-9 harbors an intermediate-mass black hole, radio and optical observations suggest that beaming and anisotropic emission from a stellar-mass black hole are unlikely to account for the implied luminosity. We further argue that the strength of the hard emission in these sources and well-established phenomena frequently observed in stellar-mass black holes near to the Eddington limit suggest that optically thick photospheres are unlikely to be the origin of the cool thermal emission in bright ultraluminous X-ray sources. For comparison to M81 X-9, we have also analyzed the previously unpublished EPIC-pn spectrum of NGC 1313 X-1; cool disk emission is again observed, and refined spectral fit parameters and mass estimates are reported.

*Subject headings:* accretion, accretion disks — black hole physics — relativity — X-rays: binaries

### 1. INTRODUCTION

Ultraluminous X-ray sources (ULXs) are pointlike X-ray sources in nearby galaxies for which the implied luminosity exceeds the Eddington limit [ $L_{\text{Edd}} = 1.3 \times 10^{38} (M/M_\odot)$  ergs  $s^{-1}$ ] for an isotropically emitting black hole of  $10 M_\odot$  (as per dynamically constrained Galactic black holes; see McClintock & Remillard 2004). A number of these sources were first identified with *Einstein* (see, e.g., Fabbiano 1989), but the spatial resolution and sensitivity of *Chandra* has shown that most ULXs are likely point sources. Short-term and longer term variability studies have shown that most ULXs must be accreting sources, likely harboring black holes feeding from companion stars in binary systems (for reviews, see Fabbiano & White 2004; Miller & Colbert 2004).

Intermediate-mass black holes (IMBHs,  $10^2\text{--}10^5 M_\odot$ ) provide an attractive explanation for ULXs. However, this interpretation requires excellent evidence that alternative explanations are unlikely to hold. Viable models for ULXs that only require stellar-mass black holes ( $\simeq 10 M_\odot$ ) and that might explain at least the lower luminosity ULXs include

anisotropic emission due to a funnel-like inner disk geometry (King et al. 2001), strongly beamed emission due to a line of sight coincident with a jet axis (Reynolds et al. 1997; Kording et al. 2002), and “slim” disks (Watarai et al. 2001) and/or radiation-pressure-dominated super-Eddington accretion disks (e.g., Begelman 2002).

While some prior analyses of X-ray spectra (e.g., with *ASCA*) found some evidence for IMBHs, the sensitivity of these observations only statistically required single-component spectral models (see Colbert & Mushotzky 1999; Makishima et al. 2000), which prevented stronger conclusions. The high effective area and sensitivity of *XMM-Newton* are changing this observational constraint (Miller et al. 2003; Strohmayer & Mushotzky 2003). Similarly, high-quality optical observations of ULXs are now being made (e.g., Pakull & Mirioni 2004) that reveal relatively symmetric nebulae around some sources with spectra indicating the ULX is acting on the local environment. The symmetry of these nebulae may indicate that these ULXs emit isotropically, and that funneling does not hold. Similarly, radio-to-X-ray flux ratios may be used to constrain relativistic beaming models. Miller et al. (2003) analyzed *XMM-Newton* EPIC-MOS spectra of the ULXs NGC 1313 X-1 and X-2. These ULX spectra were the first to statistically require thermal disk and power-law continuum components. Remarkably, the disk temperatures measured in these spectra are 5–10 times *lower* than those commonly measured in stellar-mass black holes accreting at high rates. Those temperatures, the normalization of the disk components,

<sup>1</sup> Harvard-Smithsonian Center for Astrophysics, 60 Garden Street, Cambridge, MA 02138; jmmiller@cfa.harvard.edu.

<sup>2</sup> NSF Astronomy and Astrophysics Fellow.

<sup>3</sup> Institute of Astronomy, University of Cambridge, Madingley Road, Cambridge CB3 0HA, UK.

<sup>4</sup> Department of Astronomy, University of Maryland, College Park, MD 20742.

and the very high luminosities implied suggest that NGC 1313 X-1 and X-2 may harbor IMBHs. This suggestion is strengthened by symmetric optical nebulae around X-1 and X-2 that suggest isotropic emission, and radio observations that likely rule out relativistic beaming (Miller et al. 2003). *XMM-Newton* observations of the brightest ULX in M82 reveal quasi-periodic oscillations and even an Fe K $\alpha$  emission line; the detection of these disk signatures strongly rules out beaming and likely also funneling, and also represents strong evidence that the M82 ULX may harbor an IMBH (Strohmayer & Mushotzky 2003).

The ULX M81 X-9 (actually in the dwarf galaxy Holmberg IX, but hereafter referred to as M81 X-9) is an exceptionally bright ( $L_X > 10^{40}$  ergs s $^{-1}$ ) source that is variable on the timescale of weeks and months, with weak indications for a cool disk component (La Parola et al. 2001). The source position is roughly 2' from the optical center of Ho IX.<sup>5</sup> In order to better understand the nature of M81 X-9, we analyzed spectra obtained in two short *XMM-Newton* observations available in the public archive. Herein, we report the results of fits to the *XMM-Newton* EPIC-pn spectra of M81 X-9. For comparison, we also analyzed the EPIC-pn spectrum of NGC 1313 X-1 (only the EPIC-MOS spectra were analyzed previously). Fits to these X-ray spectra suggest that both sources may harbor IMBHs. We discuss these results within the context of other recent ULX observations and prevalent models for ULX accretion flow geometries.

## 2. OBSERVATIONS AND DATA REDUCTION

In this work, we consider the time-averaged *XMM-Newton* EPIC-pn spectra gathered in two observations of M81 X-9 and a single observation of NGC 1313 X-1. The data sets were obtained through the *XMM-Newton* public data archive. The EPIC-pn camera has a higher effective area than the EPIC-MOS cameras, and drives the results of any joint spectral analysis. The results of an analysis of the EPIC-MOS spectra of NGC 1313 X-1 and X-2 are reported in Miller et al. (2003). That analysis used the *XMM-Newton* reduction and analysis suite SAS version 5.3.3, which failed to produce EPIC-pn event lists for the observation of NGC 1313. The reduction and analysis reported in this work used SAS version 5.4.2, which successfully produced an EPIC-pn event list for the NGC 1313 observation. The results of fits to the EPIC-pn spectrum of NGC 1313 X-1 (the stronger IMBH candidate of the two ULXs considered; Miller et al. 2003) are reported in this work.

M81 X-9 (Ho IX X-1) was observed on 2002 April 10 starting at 17:37:52 (UT), and again on 2002 April 16 starting at 17:33:15 (UT). In both cases, the camera was operated in “prime full window” mode, with the “thin” optical blocking filter. Application of the standard time filtering resulted in net exposures of 7.8 and 8.5 ks, respectively. In both cases, events were extracted in a circle within 24" of the source position ( $\alpha = 09^{\text{h}}57^{\text{m}}54^{\text{s}}$ ,  $\delta = 69^{\circ}03'46''$ ; La Parola et al. 2001). Because of the proximity of the source to the edge of the CCD and the relatively few bright sources apparent in the surrounding region, background counts were extracted in an adjacent circle with a radius of 24". NGC 1313 was observed by *XMM-Newton* on 2000 October 17 starting at 03:59:23 (UT). The camera was operated in prime full window mode

with the “medium” optical blocking filter. Application of the standard time filtering resulted in a net exposure of 29.3 ks. Events were extracted in a circle within 24" of the position reported by Miller et al. (2003). A background spectrum was extracted in an annulus between 24" and 30", again centered on the source position.

Each of the spectra were made by applying the selection criteria described in the MPE “cookbook.” Briefly, these selections are as follows: we set “FLAG = 0” to reject bad pixels and events too close to chip edges, event patterns 0–4 were allowed (these patterns correspond to “singles” and “doubles”), and the spectral channels were grouped by a factor of 5. The “canned” response files appropriate to the CCD, patterns, and the optical blocking filter were used to fit the data. Using the SAS tool *epatplot* and simulating *XMM-Newton* EPIC-pn spectra using the HEASARC tool PIMMS (based on prior reported fluxes and spectral parameters), we found that the effects of photon pileup are negligible in the spectra. Prior to fitting, the source and background spectra were rebinned (using *grppha* within LHEASOFT ver. 5.2) to require at least 15 counts per bin to ensure the validity of  $\chi^2$  statistical analysis. Spectral fits were made using XSPEC version 11.2.<sup>6</sup> All spectral fits were made in the 0.3–10.0 keV band. All errors reported in this work are 90% confidence errors, and were evaluated while allowing all spectral model components to vary to take account of dependencies between parameters and components. For all spectral fits, the standard *F*-test was employed to calculate the significance of adding model components.

## 3. ANALYSIS AND RESULTS

We considered a number of continuum models commonly applied to Galactic X-ray binary systems, modified by absorption in the interstellar medium using the XSPEC model *phabs*. Although somewhat technical, it is worth noting that fits to *XMM-Newton* RGS spectra of bright Galactic X-ray binaries show that *phabs* places the neutral oxygen absorption edge at an energy slightly below that expected for neutral atomic oxygen (0.543 keV). At CCD resolution, this can have the effect of creating a false emission line feature at an energy just above that which *phabs* assumes for the oxygen edge. Although different fixes for this problem are possible, we adopted the following approach (in part because it is easily reproducible). Each spectrum was fit with a model consisting of a simple power law modified by *phabs*; the edge depth expected for the neutral oxygen edge based on this column and assuming solar abundances was calculated; all continuum models then fitted to the spectra were modified by *vphabs* with the abundance of oxygen set to zero, with an additional edge fixed at the calculated depth added at 0.543 keV. Regardless of the continuum model, this absorption model proves to be a better fit to each spectrum in the region of the oxygen edge, and removes the (false) apparent emission line.

The results of all spectral fits are reported in Table 1. The spectra of M81 X-9 are shown in Figures 1, 2, 3, and 4, and the spectrum of NGC 1313 X-1 is shown in Figures 5 and 6. While a simple power law proves to be the best single-component continuum model in each case, it is only an acceptable model for the latter observation of M81 X-9. The

<sup>5</sup> Data from the LEDA database, which is available at <http://www-obs.univ-lyon1.fr/hypercat/leda>.

<sup>6</sup> XSPEC is available from HEASARC at <http://heasarc.gsfc.nasa.gov/docs/software/lheasoft/source.html>. The HEASARC on-line service is provided by the NASA Goddard Space Flight Center.

TABLE 1  
SPECTRAL FIT PARAMETERS

| Model Parameter  | M81 X-9 Obs. 1         | M81 X-9 Obs. 2         | NGC 1313 X-1           |
|--|------------------------|------------------------|------------------------|
| Power-Law Model  |                        |                        |                        |
| $N_{\text{H}}$ ( $10^{21}$ cm $^{-2}$ ).....           | 2.1 (1)                | 2.5 (2)                | 2.4 (2)                |
| $\Gamma$ .....   | 1.93 (4)               | 2.00 (4)               | 2.04 (5)               |
| Norm. ( $10^{-3}$ ).....                               | 1.24 (4)               | 1.57 (5)               | 0.69 (3)               |
| $\chi^2/\text{dof}$ .....                              | 460.7/443              | 571.7/579              | 555.7/489              |
| MCD Model  |                        |                        |                        |
| $N_{\text{H}}$ ( $10^{21}$ cm $^{-2}$ ).....           | 2.1                    | 2.5                    | 2.4                    |
| $kT$ (keV).....  | 0.91 (5)               | 1.63 (4)               | 0.78 (5)               |
| Norm. ( $10^{-1}$ ).....                               | 3.5 (2)                | 0.40 (2)               | 3.2 (2)                |
| $\chi^2/\text{dof}$ .....                              | 1823/444               | 1421/579               | 1919/490               |
| Bremsstrahlung Model                                   |                        |                        |                        |
| $N_{\text{H}}$ ( $10^{21}$ cm $^{-2}$ ).....           | 2.1                    | 2.5                    | 2.4                    |
| $kT$ (keV).....  | 31 (1)                 | 43 (1)                 | 4.6 (1)                |
| Norm. ( $10^{-3}$ ).....                               | 1.04 (2)               | 1.22 (2)               | 0.70 (2)               |
| $\chi^2/\text{dof}$ .....                              | 1510/443               | 2435/579               | 773/489                |
| MCD + Power Law Model                                  |                        |                        |                        |
| $N_{\text{H}}$ ( $10^{21}$ cm $^{-2}$ ).....           | 2.3 (3)                | 2.9 (3)                | 3.1 (3)                |
| $kT$ (keV).....  | $0.26^{+0.02}_{-0.05}$ | 0.21 (4)               | 0.23 (2)               |
| Norm. ....   | $20^{+20}_{-10}$       | $60^{+70}_{-40}$       | 28 (5)                 |
| $\Gamma$ .....   | 1.73 (8)               | 1.86 (6)               | 1.76 (7)               |
| Norm. ( $10^{-3}$ ).....                               | 0.96 (9)               | $1.34^{+0.09}_{-0.05}$ | 0.49 (4)               |
| $\chi^2/\text{dof}$ .....                              | 419.0/441              | 524.3/577              | 459.8/487              |
| Disk significance.....                                 | 6.1 $\sigma$           | 6.8 $\sigma$           | >8 $\sigma$            |
| $F$ ( $10^{-12}$ ergs cm $^{-2}$ s $^{-1}$ ).....      | $8^{+2}_{-1}$          | $10^{+2}_{-1}$         | 4.3 (4)                |
| $F_{\text{power law}}/F_{\text{total}}$ .....          | 0.85                   | 0.84                   | 0.74                   |
| $L_{0.3-10}$ ( $10^{40}$ ergs s $^{-1}$ ).....         | $1.1^{+0.3}_{-0.1}$    | $1.3^{+0.3}_{-0.2}$    | 0.6 (1)                |
| $L_{0.05-100}$ ( $10^{40}$ ergs s $^{-1}$ ).....       | $2.7^{+0.7}_{-0.3}$    | $2.9^{+0.6}_{-0.3}$    | $1.4^{+0.2}_{-0.2}$    |
| $M_{kT=1.0}$ ( $M_{\odot}$ ).....                      | $2000^{+3000}_{-1000}$ | $5000^{+7000}_{-2000}$ | $4000^{+2000}_{-1000}$ |
| $M_{kT=0.5}$ ( $M_{\odot}$ ).....                      | $140^{+180}_{-40}$     | $320^{+430}_{-160}$    | $220^{+100}_{-60}$     |
| $M_{\text{Norm}}$ ( $M_{\odot}$ ).....                 | $330^{+140}_{-100}$    | $570^{+270}_{-240}$    | $400^{+40}_{-40}$      |
| $M_{L_{\text{X}}/L_{\text{Edd}}}$ ( $M_{\odot}$ )..... | $200^{+50}_{-30}$      | $220^{+40}_{-20}$      | $110^{+10}_{-10}$      |
| diskpn + Power Law Model                               |                        |                        |                        |
| $N_{\text{H}}$ ( $10^{21}$ cm $^{-2}$ ).....           | 2.3 (3)                | 2.8 (3)                | 3.0 (3)                |
| $kT$ (keV).....  | 0.24 (5)               | 0.21 (4)               | 0.22 (3)               |
| Norm. ( $10^{-4}$ ).....                               | $4^{+16}_{-2}$         | $7^{+30}_{-3}$         | $0.5^{+0.5}_{-0.2}$    |
| $\Gamma$ .....   | $1.74^{+0.07}_{-0.04}$ | 1.85 (6)               | 1.76 (7)               |
| Norm. ( $10^{-3}$ ).....                               | 1.0 (1)                | $1.3^{+0.2}_{-0.1}$    | 0.49 (5)               |
| $\chi^2/\text{dof}$ .....                              | 418.8/441              | 524.9/577              | 461.0/487              |
| Disk significance.....                                 | 5.9 $\sigma$           | 6.7 $\sigma$           | >8 $\sigma$            |
| $F$ ( $10^{-12}$ ergs cm $^{-2}$ s $^{-1}$ ).....      | $8^{+2}_{-1}$          | $10^{+2}_{-1}$         | 4.3 (4)                |
| $F_{\text{power law}}/F_{\text{total}}$ .....          | 0.85                   | 0.85                   | 0.74                   |
| $L_{0.3-10}$ ( $10^{40}$ ergs s $^{-1}$ ).....         | $1.1^{+0.3}_{-0.1}$    | $1.3^{+0.3}_{-0.2}$    | 0.6 (1)                |
| $L_{0.05-100}$ ( $10^{40}$ ergs s $^{-1}$ ).....       | $2.7^{+0.7}_{-0.3}$    | $2.9^{+0.6}_{-0.3}$    | $1.4^{+0.2}_{-0.2}$    |
| $M_{kT=1.0}$ ( $M_{\odot}$ ).....                      | $3000^{+5000}_{-2000}$ | $5000^{+7000}_{-2000}$ | $4000^{+3000}_{-2000}$ |
| $M_{kT=0.5}$ ( $M_{\odot}$ ).....                      | $200^{+300}_{-100}$    | $300^{+400}_{-100}$    | $300^{+200}_{-100}$    |
| $M_{\text{Norm}}$ ( $M_{\odot}$ ).....                 | $330^{+20}_{-20}$      | $380^{+20}_{-20}$      | $240^{+10}_{-20}$      |
| $M_{L_{\text{X}}/L_{\text{Edd}}}$ ( $M_{\odot}$ )..... | $200^{+50}_{-30}$      | $220^{+40}_{-20}$      | $110^{+10}_{-10}$      |

NOTES.—The results of fitting simple models to the EPIC-pn spectra of M81 X-9 and NGC 1313 X-1. The XSPEC model *vphabs* was used to measure the equivalent neutral hydrogen column density along the line of sight. All errors reported above are 90% confidence errors. The significance of adding disk components was calculated using the standard  $F$ -test. Errors in parentheses are the error in the last digit. Fluxes are “unabsorbed” fluxes, and the reported luminosities assume a distance of 3.4 Mpc for Ho IX and 3.7 Mpc for NGC 1313. Mass estimates based on scaling the inner disk temperatures to those commonly measured in  $10 M_{\odot}$  black holes accreting at high rates assume  $T \propto M_{\text{BH}}^{-1/4}$ . Scalings are given assuming typical inner disk temperatures of  $kT = 1.0$  and  $0.5$  keV, although the literature favors the former. Please see the text for details on mass estimates obtained through the disk component normalizations. Mass estimates based on the Eddington luminosity make use of the  $0.05$ – $100$  keV luminosity (extrapolated from the  $0.3$ – $10.0$  keV flux) and assume  $L_{\text{Edd}} = 1.3 \times 10^{38}$  ( $M/M_{\odot}$ ) ergs s $^{-1}$ .

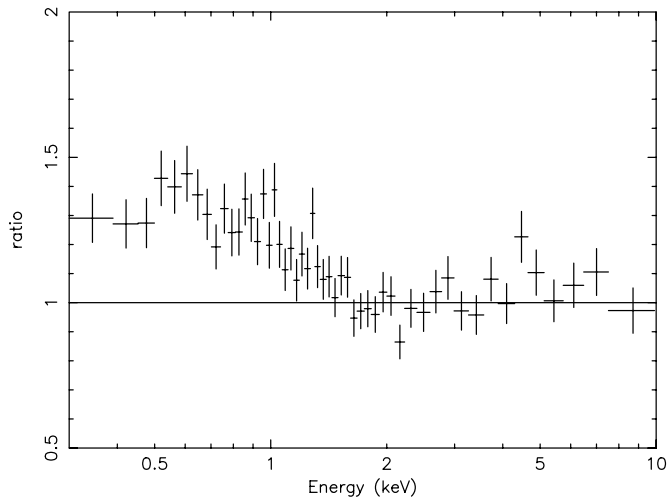


FIG. 1.—Ratio of the EPIC-pn spectrum of M81 X-9 obtained in the first observation to a model consisting of only power-law continuum fitted in the 3.0–10.0 keV band. The soft continuum excess is readily apparent at low energy. The spectrum shown has been rebinned for visual clarity.

canonical multicolor disk (MCD) blackbody model (Mitsuda et al. 1984), an approximation to the Shakura & Sunyaev (1973) disk model, is not an acceptable fit to any of the spectra when it is the only continuum component. Similarly, single-component thermal bremsstrahlung models are not an acceptable fit to any of the spectra. Although not listed in Table 1, single-component fits with any diffuse thermal plasma model are not acceptable; this is expected given the lack of emission lines in any spectrum.

Following Miller et al. (2003), we proceeded to consider two-component continuum models: MCD plus power law, *diskpn* plus power law, and MEKAL plus power law. While the MCD model is convenient in that (1) it is a common component in published fits to Galactic black hole binary spectra and (2) its temperature and normalization allow scaling from which constraints on the mass of the accretor in ULXs may be estimated, it is an approximation to the Shakura & Sunyaev (1973) disk in that it does not include the zero-torque inner boundary condition. The *diskpn* model is a disk model that includes corrections (based on a pseudo-Newtonian

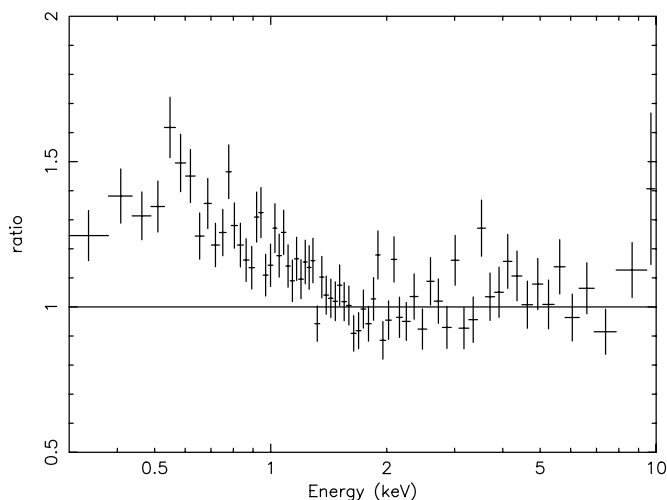


FIG. 2.—Same as Fig. 1, but for the spectrum of M81 X-9 obtained in the second observation.

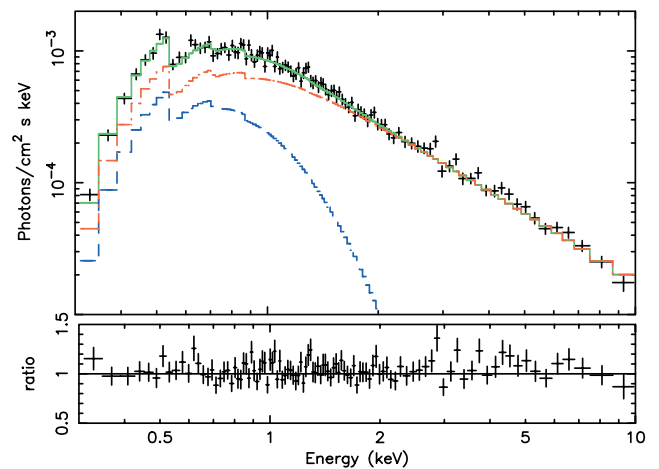


FIG. 3.—EPIC-pn spectrum of M81 X-9 obtained in the first observation of the source. The spectrum has been fitted with a model consisting of MCD (blue) and power-law (red) continuum components, and the data/model ratio is shown below. The shape of the disk component and ratio plot are nearly identical if the *diskpn* disk model is fitted instead of the MCD model. See Table 1 for details of the spectral model.

potential) for the temperature behavior near to the black hole (Gierlinski et al. 1999). As with the MCD model, the temperature and normalization parameters in this model permit scalings that can be used to constrain the mass of the accretor in ULXs. In addition, the inner disk radius is also a free parameter in the *diskpn* model ( $R_{\text{in}} = 6R_g$  was fixed in all fits, where  $R_g = GM/c^2$ ). The MEKAL model describes diffuse thermal plasmas; the results of fits with this model are not listed in Table 1 since the density parameter of this model is totally unconstrained (which is likely due to the total lack of credible emission lines in the spectra), and because MEKAL-plus-power-law models prove to be significantly worse than disk-plus-power-law models. This is particularly clear in the case of NGC 1313 X-1: the best-fit MEKAL-plus-power-law model gives  $\chi^2/\nu = 499.0/486$  (where  $\nu$  is the number of degrees of freedom); this is significantly worse than fits with a model consisting of an MCD plus power-law components ( $\chi^2/\nu = 459.8/487$ ) or a *diskpn* plus power-law components ( $\chi^2/\nu = 461.0/487$ ). Finally, it is worth noting that archival observations suggest that NGC 1313 X-1 and M81 X-9 are not

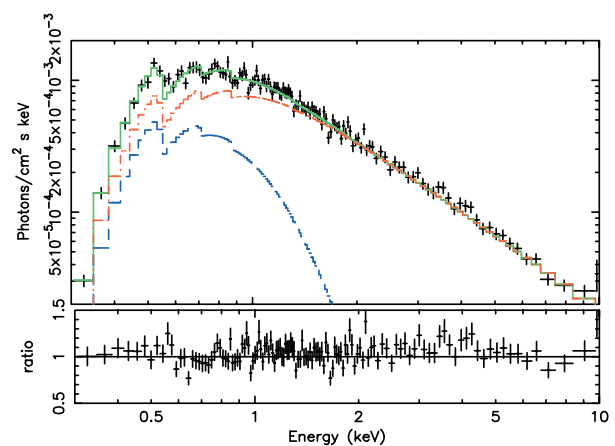


FIG. 4.—Same as Fig. 3, but for the spectrum of M81 X-9 obtained in the second observation.

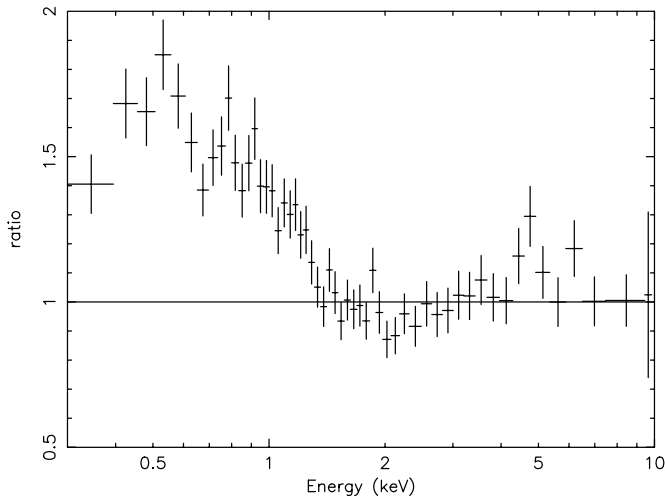


FIG. 5.—Same as Fig. 1, but for the spectrum of NGC 1313 X-1 obtained in the second observation.

diffuse sources, but are consistent with point sources at *Chandra* resolution (after accounting for pileup).

Cool disk components are formally statistically required to fit the first spectrum of M81 X-9 (the addition of a disk component is significant at the  $6\sigma$  level of confidence) and the spectrum of NGC 1313 X-1 (the addition of a disk component is significant at more than the  $8\sigma$  level of confidence). Figure 2 clearly shows that there is also excess soft emission in the second spectrum of M81 X-9. It was shown previously that soft excesses of this kind are robust against underabundances in the local absorbing material (Miller et al. 2003), and that result holds for these spectra as well. When a disk component is included in the model, the parameters of the disk component can be constrained and the addition gives an improvement that is significant at nearly the  $7\sigma$  level. Remarkably, the disk components in fits to M81 X-9 yield very low temperatures (ranging between  $kT = 0.17$ – $0.29$  keV, including 90% confidence errors, and considering each of the two models fitted to the two observations of M81 X-9). Inner disk temperatures ranging between  $kT = 0.21$  and  $0.25$  keV are measured for the disk component in the spectrum of NGC 1313 X-1. The power-law indices measured are harder than those commonly measured in the “very high” state in stellar-mass Galactic black holes, but softer than those commonly measured in the “low/hard” state.

Estimates for the mass of the black holes in M81 X-9 and NGC 1313 X-1 are given in Table 1, based on three independent methods: (1) scaling the inner disk temperature to values commonly measured in Galactic black holes, (2) direct estimates from the normalization of the disk components, and (3) scaling from the Eddington limit equation.

At the highest mass accretion rates observed in stellar-mass black holes, inner disk temperatures near to or above  $kT = 1$  keV are often observed (for a review, see McClintock & Remillard 2004; for a recent example, see Park et al. 2004). In some cases, however, the inner disk temperatures can be as high as  $kT \approx 2$  keV (for examples and a comparison to ULXs, see Makishima et al. 2000). Using the fact that in blackbody disk models,  $T \propto M^{-1/4}$ , it is possible to scale temperature to mass via the relation  $(M_{\text{ULX}}/M_{10 M_{\odot}}) \propto (kT_{10 M_{\odot}}/kT_{\text{ULX}})^4$ . Assuming that M81 X-9 and NGC 1313 X-1 are accreting at or near to the Eddington limit (the regime in which hot disks are

observed in stellar-mass Galactic black holes), this scaling suggests that these ULXs harbor black holes with masses of few  $\times 10^3 M_{\odot}$  (see Table 1). Clearly, this scaling is very sensitive to what temperature is assumed to be typical of stellar-mass Galactic black holes accreting at high rates. Assuming  $kT = 0.5$  keV to be typical gives masses of few  $\times 10^2 M_{\odot}$  for M81 X-1 and NGC 1313 X-1; however, assuming  $kT = 1.0$  keV to be typical for stellar-mass black holes accreting at or near to the Eddington limit has a much stronger observational basis.

The MCD and *diskpn* normalizations also allow estimates of the black hole masses. In this case, some care is required because it has been noted that the color temperature measured using MCD models may differ from the effective temperature (Shimura & Takahara 1995; Merloni et al. 2000). Whereas corrections divide out in scaling the temperature, they must be considered in scaling masses from the disk-component normalization. The MCD normalization gives the inner disk extent in kilometers, which can be converted into a black hole mass. Following recent related work (Miller et al. 2003; see also Sobczak et al. 2000 and Makishima et al. 2000), we take  $R_{\text{in,corr}} = \eta f^2 R_{\text{obs}}$  for the MCD model (where  $f = 1.7$  is the spectral hardening factor, and  $\eta = 0.63$  is valid for  $i < 70^\circ$  and accounts for the difference between the innermost radius and the radius of peak temperature; note also that in all disk normalization scalings we assumed  $i = 0$  and that any higher inclination gives a *higher* mass). For a Schwarzschild black hole,  $R_{\text{in}} = 6R_g = 8.85 \text{ km } M_{\odot}^{-1}$  (where  $R_g = GM/c^2$ ). Therefore, we can use the MCD model to obtain mass estimates via the relation

$$M_{\text{ULX}} = \eta f^2 [K / \cos(i)] (d/10 \text{ kpc}) \times (8.85 \text{ km})^{-1},$$

where  $K$  is the MCD normalization,  $i$  is the inclination, and  $d$  is the source distance. Assuming distances of  $d = 3.4$  Mpc for Ho IX (Georgiev et al. 1991; Hill et al. 1993) and  $d = 3.74$  Mpc for NGC 1313 (Tully 1988), the MCD component normalization suggests that M81 X-9 and NGC 1313 X-1 may harbor black holes with masses of few  $\times 10^2 M_{\odot}$  (see Table 1). The normalization of the *diskpn* component explicitly includes the mass and the color correction factor  $f$ . In estimating masses with the *diskpn* model,  $f = 1.7$  was again

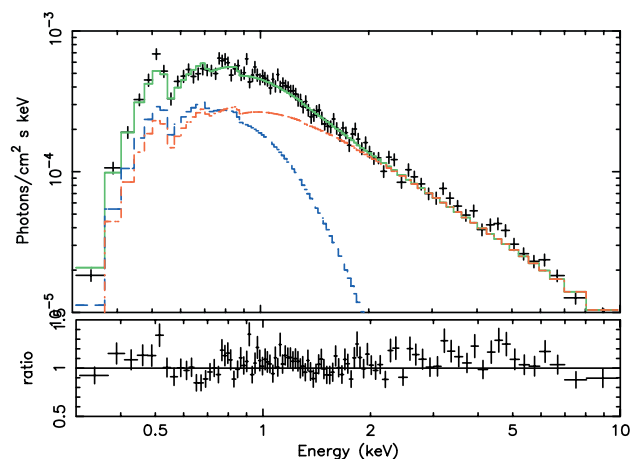


FIG. 6.—Same as Fig. 3, but for the spectrum of NGC 1313 X-1 obtained in the first observation.

assumed, as per the MCD model. The *diskpn* normalizations measured for M81 X-9 and NGC 1313 X-1 again suggest that these ULXs may harbor black holes with masses of few  $\times 100 M_{\odot}$  (see Table 1).

The mass of the putative black holes powering M81 X-9 and NGC 1313 X-1 can also be estimated by scaling the implied source luminosities to the Eddington limit for isotropically emitting accretion-powered sources [ $L_{\text{Edd}} = 1.3 \times 10^{38} (M/M_{\odot}) \text{ ergs s}^{-1} M_{\odot}^{-1}$ ; Frank et al. 2002]. To make this scaling, the unabsorbed 0.3–10.0 keV flux was extrapolated to the 0.05–100.0 keV band, since the latter is more representative of a bolometric luminosity. This scaling again implies that M81 X-9 and NGC 1313 X-1 may harbor black holes with masses of few  $\times 10^2 M_{\odot}$  (see Table 1). It is interesting to note that scaling the ULX inner disk temperatures to  $kT = 1.0 \text{ keV}$  implies masses on the order of  $10^3 M_{\odot}$ , while the disk normalizations and overall luminosities imply masses on the order of  $10^2 M_{\odot}$ . This may imply that these ULXs are  $10^3 M_{\odot}$  black holes seen at  $L_X \simeq 0.1 \times L_{\text{Edd}}$ .

Finally, we note that while the results obtained here for NGC 1313 X-1 broadly agree with those previously reported in Miller et al. (2003), they do not agree exactly. The differences can be attributed to several factors, including the more conservative fitting range used in this analysis (0.3–10.0 keV) relative to the prior analysis, the higher effective area, sensitivity, and energy resolution of the EPIC-pn camera (used in this analysis) relative to the EPIC-MOS cameras (used in the prior analysis), and the improved interstellar absorption model used in this analysis. The most important difference is that the disk temperatures measured in this analysis are 0.08 keV higher than in the previous analysis ( $kT = 0.23 \text{ keV}$  vs.  $kT = 0.15 \text{ keV}$ ), resulting in new mass estimates that are 5 times lower than prior estimates using inner disk temperatures.

#### 4. DISCUSSION

We have investigated the nature of the ULX M81 X-9 (Holmberg IX X-1) by analyzing two *XMM-Newton* EPIC-pn spectra of the source. The most important result of this work is that cool thermal continuum emission is unambiguously required for the first time. Optically thick disk components yield improvements in the fit statistic that are significant at more than the  $6 \sigma$  level of confidence. This represents the clearest evidence for a cool accretion disk in a ULX apart from that for NGC 1313 X-1 (Miller et al. 2003; see Table 1).

Remarkably, the inner disk temperatures measured ( $kT = 0.17\text{--}0.29 \text{ keV}$ , including 90% confidence errors on two disk models fitted to the two observations) are well below those commonly measured in stellar-mass black holes ( $kT \simeq 1 \text{ keV}$ ; see McClintock & Remillard 2004 for a review). Scaling the temperatures measured implies that M81 X-9 may harbor a black hole with a mass on the order of  $10^3 M_{\odot}$ , and scaling the disk component normalizations implies masses on the order of  $10^2 M_{\odot}$ . It is unclear which scaling method is superior, but both scalings suggest that M81 X-9 may harbor an IMBH. Both scaling methods can be correct if the source harbors a black hole with a mass on the order of  $10^3 M_{\odot}$  that is observed at  $L_X \simeq 0.1 \times L_{\text{Edd}}$ . For comparison, we also report results from an analysis of the EPIC-pn spectrum of NGC 1313 X-1, which may also harbor an IMBH (Miller et al. 2003). The spectra of these sources bear striking similarities (see Table 1).

The long- and short-term flux variability of M81 X-9 demonstrated clearly by La Parola et al. (2001) establishes

that M81 X-9 is an accreting source. While it is natural to ascribe cool thermal emission to an optically thick accretion disk in accreting systems, given the implications of these cool disks it is especially important to understand why disk emission is the most viable explanation.

Relativistic beaming (which might prevent detection of disk signatures) is not likely at work in M81 X-9. First, radio observations of Ho IX by Bash & Kaufman (1986) find a flux density of at most 1 mJy at 20 cm at the position of the ULX, corresponding to a luminosity of  $\simeq 2 \times 10^{34} \text{ ergs s}^{-1}$ . If the source was active at its present level during that time (as suggested by the long-term behavior reported by La Parola et al. 2001), this radio luminosity gives a radio-to-X-ray luminosity ratio of  $\simeq 2 \times 10^{-6}$ . This is at odds with a relativistic beaming scenario, as beaming should create flat spectra (see, e.g., Fossati et al. 1998). Second, the peak radio-to-X-ray flux ratios observed in Galactic X-ray binary systems are always below  $2.3 \times 10^{-5}$  (Fender & Kuulkers 2001; Barth et al. 2004). The fact that the radio-to-X-ray flux ratio in M81 X-9 is likely an order of magnitude below the highest ratio seen in Galactic systems suggests that M81 X-9 is not likely to be a stellar-mass black hole with relativistically beamed emission coincident with our line of sight to the source.

Slightly anisotropic X-ray emission, perhaps due to a funnel-like geometry in the inner disk, might create a very hot inner disk, especially if the source of hard X-ray emission is central (e.g., through Comptonization). Clearly, the spectra we have analyzed rule out hot-disk signatures. Pakull & Mirioni (2004) have reported optical nebulae around a few ULXs, including NGC 1313 X-1 and M81 X-9. The line ratios observed in these nebulae suggest that X-ray photoionization may be important, and hint that some ULXs may act on their local interstellar medium. The symmetry of the nebula around NGC 1313 X-1 suggests that the source emits isotropically. While the nebula imaged around M81 X-9 is better described by an ellipse than a circle, the ratio of the axes is likely less than 2:1, and is certainly inconsistent with a ratio of 10:1 (“funneled” scenarios require an anisotropy parameter of approximately 10; see King et al. 2001). Thus, present data suggests that anisotropic emission is not the best explanation for the high flux observed from M81 X-9.

Radiation pressure-dominated accretion disks, which might be able to produce super-Eddington fluxes through small-scale photon bubble instabilities (Begelman 2002), might be expected to have especially high temperatures (perhaps similar to the “slim” disk solution described by Watarai et al. 2001). As the spectra of M81 X-9 and NGC 1313 X-1 are inconsistent with hot-disk components, it is not likely that such models describe these sources.

Finally, it has recently been suggested that soft thermal emission in the brightest ULXs may be due to an optically thick, outflowing photosphere originating at  $100 R_{\text{Schw}}$  around a stellar-mass black hole accreting at a super-Eddington rate (e.g., King 2003). This model is inconsistent with the relative importance of hard X-ray emission in sources such as M81 X-9 and NGC 1313 X-1. It is also inconsistent with a number of long-established properties observed in stellar-mass Galactic black holes accreting near to, at, or slightly in excess of their isotropic Eddington luminosities. We briefly consider these issues here.

The mechanical power in a photosphere outflowing at velocity  $v$  should scale with the luminosity radiated by the photosphere as  $L_{\text{mech}} \simeq L_{\text{rad}}(v/c)$ , and the photospheric radius is given by  $R_{\text{phot}} \simeq (c/v)^2 R_{\text{Schw}}$  (King 2003). Hard X-ray

emission in accreting sources is usually tied to regions deep within the gravitational potential, as this is a convenient energy reservoir. However, the innermost accretion regime would be blocked from view by an optically thick photosphere. The observed hard component in such a scenario must be generated in shocks above the photosphere, which means that the strength of the hard component must be driven by the outflow:  $L_{\text{hard}} \simeq L_{\text{mech}}$ . Measurements indicate that the hard components in M81 X-9 and NGC 1313 X-1 are 3–4 times stronger than the soft (putatively photospheric) components in each spectrum (see Table 1). Even if we only assume that  $L_{\text{hard}} \simeq L_{\text{soft}} \simeq L_{\text{rad}}$ , the only way  $L_{\text{mech}} \simeq L_{\text{rad}}(v/c)$  holds is if  $(v/c) \simeq 1$ , which implies that  $R_{\text{phot}} \simeq (c/v)^2 R_{\text{Schw}} \simeq 1 R_{\text{Schw}}$ .

Moreover, even at the highest implied accretion rates a number of spectral and variability properties observed in stellar-mass Galactic black holes would be screened if an optically thick photosphere developed at  $R_{\text{phot}} \simeq 100 R_{\text{Schw}}$ . First, hot ( $kT \simeq 1$  keV) thermal spectral components are observed in every source at peak X-ray flux; this emission can only be associated with the inner disk since a radially distant photosphere should be much cooler. Second, QPOs, whether high frequency (few  $\times 100$  Hz) or low frequency (few  $\times 1$  Hz), are almost certainly tied to the disk and likely represent Keplerian orbital frequencies and/or coordinate resonance frequencies. QPOs are seen over a factor of  $10^3$  in flux in stellar-mass Galactic black holes but are preferentially seen at high fluxes. Most importantly, QPOs are a higher fraction of the rms noise at high energies: QPOs are intimately tied to hard X-ray emission. It is very unlikely that such periodicities originate in shocks above an optically thick photosphere. Third, broad relativistic Fe  $K\alpha$  emission lines are also observed in stellar-mass Galactic black holes over a factor of  $10^3$  in flux, but preferentially at the very highest fluxes (e.g., in the very high state). These lines are certainly tied to hard X-ray emission (see, e.g., Zdziarski et al. 1999), and have been observed to vary at frequencies as high as 6 Hz (Gilfanov et al. 2000). These facts, and their smeared shape (very likely due to the extreme Doppler shifts and gravitational redshift at the inner disk), tie broad Fe  $K\alpha$  emission lines to the innermost accretion flow. The reader is directed to McClintock & Remillard (2004) and references therein for a discussion of the stellar-mass black hole properties noted here.

It is worth noting that partial covering models for NGC 1313 X-1 and M81 X-9 cannot be ruled out statistically in the limited energy range considered. Models consisting of a strong absorber ( $N_{\text{H}} \simeq 10^{23} \text{ cm}^{-2}$ ) covering 50%–70% of a steep power-law source ( $\Gamma \simeq 2.7$ ) can fit the data as well as our disk-plus-power-law models. There are several reasons, however, why partial covering is likely an unphysical model for these sources. First, partial covering is only required in Galactic black hole sources during X-ray “dips” (e.g., 4U 1630–472 and GRO J1655–40; Kuulkers et al. 1998). When partial covering is actually required to fit the spectra of Galactic black holes and active galactic nuclei (AGNs), fits with simple models require very strong neutral Fe K absorption edges: Ueda et al. (1998) find an edge with  $\tau = 3.3$  in GRO J1655–40, and Boller et al. (2002) report an edge with  $\tau = 1.8$  in 1H 0707–495. In contrast, X-ray dips have never been observed in NGC 1313 X-1 or M81 X-9, and the 95% confidence upper limits on the strength of a neutral Fe K edges in the spectra of NGC 1313 X-1 and M81 X-9 are  $\tau \leq 0.4$  and  $\tau \leq 0.2$ , respectively. Next, it has been shown that while partial covering models can provide acceptable fits to AGN data below 10 keV, simultaneous high-energy spectra strongly

reject such models (see, e.g., Reynolds et al. 2004). Finally, the above discussion of photospheric models shows that an alternative geometry wherein partial covering might arise naturally is very unlikely to describe sources such as NGC 1313 X-1 and M81 X-9.

Thus, at present the most viable explanation for the soft thermal excess observed in sources such as M81 X-9 and NGC 1313 X-1 is emission from a cool accretion disk around an IMBH. Recent observations of bright ULXs with *XMM-Newton* and *Chandra* have revealed cool thermal (likely disk) components in a number of ULXs, including (but not limited to) NGC 1313 X-1 and X-2 (Miller et al. 2003), NGC 5408 X-1 (Kaaret et al. 2003), NGC 4038/4039 X-37 (Miller et al. 2004), and M74 X-1 (Krauss et al. 2004). The brightest ULX in M82 may or may not have a cool disk; the low-energy portion of the spectrum from that ULX has proved difficult to measure because of photon pileup in CCD spectrometers (with *Chandra*) and diffuse emission in the crowded field (with *XMM-Newton*). However, beaming is confidently ruled out in this source through the observation of QPOs and an Fe  $K\alpha$  emission line (Strohmer & Mushotzky 2003), and this source is an excellent IMBH candidate. At most, these observations suggest that sources at the upper end of the ULX luminosity distribution may harbor IMBHs. Many ULXs at the lower end of the luminosity distribution may be stellar-mass black holes. As observations of ULXs continue to be made (especially multiwavelength observations), it is likely that subclasses of beamed, funneled, and IMBH sources will be distinguished.

If M81 X-9 harbors an IMBH, we can speculate about how such a black hole was made. This speculation is particularly interesting because Ho IX is a dwarf galaxy. Madau & Rees (2001) have proposed that IMBHs might have been created by the death of extremely massive low-metallicity Population III stars. While most IMBHs created in this way may have been dragged to galactic centers by dynamical friction, a fraction might be visible today as ULXs if they have captured a donor star. If M81 X-9 has a mass on the order of  $10^2 M_{\odot}$  and this scenario can hold in the case of dwarf galaxies, M81 X-9 could be a Population III remnant. If M81 X-9 has a mass on the order of  $10^3 M_{\odot}$ , it is more likely that it grew through mergers, either in a young cluster (e.g., Ebisuzaki et al. 2001) or in a globular cluster (Miller & Hamilton 2002). Certainly, Miller (1995) notes that the vicinity of M81 X-9 may contain a number of massive young stars, and may show evidence for a recent supernova history.

We wish to thank the referee for helpful suggestions. J. M. M. acknowledges support from the NSF through its Astronomy and Astrophysics Postdoctoral Fellowship program. M. C. M. was supported in part by NSF grant AST 00-98436 and by NASA grant NAG 5-13229. This work is based on observations obtained with *XMM-Newton*, an ESA mission with instruments and contributions directly funded by ESA member states and the US (NASA). This work has made use of the tools and services available through HEASARC on-line service, which is operated by the Goddard Space Flight Center for NASA. The authors note for the curious that J. M. Miller (Miller et al. 2003, 2004), M. C. Miller (Miller & Hamilton 2002; Miller & Colbert 2004), and B. F. Miller (Miller 1995) are indeed distinct, unrelated people.

## REFERENCES

- Barth, A. J., Ho, L. C., & Sargent, W. L. W. 2004, in ASP Conf. Ser. 311, AGN Physics with the Sloan Digital Sky Survey, ed. G. T. Richards & P. B. Hall (San Francisco: ASP), in press
- Bash, F. N., & Kaufman, M. 1986, ApJ, 310, 621
- Begelman, M. 2002, ApJ, 568, L97
- Boller, T., et al. 2002, MNRAS, 329, L1
- Colbert, E. J. M., & Mushotzky, R. F. 1999, ApJ, 519, 89
- Ebisuzaki, T., et al. 2001, ApJ, 562, L19
- Fabbiano, G. 1989, ARA&A, 27, 87
- Fabbiano, G., & White, N. E. 2004, in Compact Stellar X-Ray Sources, ed. W. H. G. Lewin & M. van der Klis (Cambridge: Cambridge Univ. Press), in press (astro-ph/0307142)
- Fender, R. P., & Kuulkers, E. 2001, MNRAS, 324, 923
- Fossati, G., Maraschi, L., Celotti, A., Comastri, A., & Ghisellini, G. 1998, MNRAS, 299, 433
- Frank, J., King, A. R., & Raine, D. 2002, Accretion Power in Astrophysics (Cambridge: Cambridge Univ. Press)
- Georgiev, T. B., Bilkina, B. I., Tikhonov, N. A., & Karachentsev, I. 1991, A&AS, 89, 529
- Gierlinski, M., Zdziarski, A. A., Poutanen, J., Coppi, P. S., Ebisawa, K., & Johnson, W. N. 1999, MNRAS, 309, 496
- Gilfanov, M., Churazov, E., & Revnivtsev, M. 2000, MNRAS, 316, 923
- Hill, J. K., et al. 1993, ApJ, 402, L45
- Kaaret, P., Corbel, S., Prestwich, A. H., & Zezas, A. 2003, Science, 299, 365
- King, A. R., 2003, Proc. 2nd *BeppoSAX* Meeting, The Restless High-Energy Universe, ed. E. P. J. van den Heuvel, J. J. J. M. in 't Zand, & R. A. M. J. Wijers, preprint (astro-ph/0309524)
- King, A. R., Davies, M. B., Ward, M. J., Fabbiano, G., & Elvis, M. 2001, ApJ, 552, L109
- Kording, E., Falcke, H., & Markoff, S. 2002, A&A, 382, L13
- Krauss, M., et al. 2004, ApJ, in press
- Kuulkers, E., Wijnands, R., Belloni, T., Mendez, M., van der Klis, M., & van Paradijs, J. 1998, ApJ, 494, 753
- La Parola, V., Peres, G., Fabbiano, G., Kim, D. W., & Bocchino, F. 2001, ApJ, 556, 47
- Madau, P., & Rees, M. J. 2001, ApJ, 551, L27
- Makishima, K., et al. 2000, MNRAS, 313, 193
- McClintock, J. E., & Remillard, R. A. 2004, in Compact Stellar X-Ray Sources, ed. W. H. G. Lewin & M. van der Klis (Cambridge: Cambridge Univ. Press), in press (astro-ph/0306213)
- Merloni, A. A., Fabian, A. C., & Ross, R. R. 2000, MNRAS, 313, 193
- Miller, B. F. 1995, ApJ, 446, L75
- Miller, J. M., Fabbiano, G., Miller, M. C., & Fabian, A. C. 2003, ApJ, 585, L37
- Miller, J. M., Zezas, A., Fabbiano, G., & Schweizer, F. 2004, ApJ, in press (astro-ph/0302535)
- Miller, M. C., & Colbert, E. J. M., 2004, Int. J. Mod. Phys. D., 13, 1
- Miller, M. C., & Hamilton, D. P. 2002, MNRAS, 330, 232
- Mitsuda, K., et al. 1984, PASJ, 36, 741
- Pakull, M. W., & Mirioni, L., 2004, in New Visions of the X-Ray Universe in the *XMM-Newton* and *Chandra* Era (ESA SP-488; Noordwijk: ESA), in press (astro-ph/0202488)
- Park, S. Q., et al. 2004, ApJ, in press (astro-ph/0308363)
- Reynolds, C. S., Loan, A. J., Fabian, A. C., Makishima, K., Brandt, W. N., & Mizuno, T. 1997, MNRAS, 286, 349
- Reynolds, C. S., Wilms, J., Begelman, M. C., Staubert, R., & Kendziorra, E. 2004, MNRAS, in press (astro-ph/0401305)
- Shakura, N. I., & Sunyaev, R. A. 1973, A&A, 24, 337
- Shimura, T., & Takahara, F. 1995, ApJ, 445, 780
- Sobczak, G. J., et al. 2000, ApJ, 544, 993
- Strohmayer, T. E., & Mushotzky, R. F. 2003, ApJ, 586, L61
- Tully, R. B. 1988, Nearby Galaxies Catalog (Cambridge: Cambridge Univ. Press)
- Ueda, Y., Inoue, H., Tanaka, Y., Ebisawa, K., Nagase, F., Kotani, T., & Gehrels, N. 1998, ApJ, 492, 782
- Watarai, K., Mizuno, T., & Mineshige, S. 2001, ApJ, 549, L77
- Zdziarski, A. A., Lubinski, P., & Smith, D. A. 1999, MNRAS, 303, L11